Journal of Neonatal Surgery
ISSN(Online): 2226-0439
Vol. 14, Issue 32s (2025)
https://www.jneonatalsurg.com

OPEN ACCESS

Improved Empirical Wavelet Transform Based Signal Preprocessing And Attention-Based Residual Optimized Bilstm (AROBILSTM) Classifier For Epileptic Seizure Detection

Ramya.K[1], Dr. M.Kokilamani[2]

[1] Research Scholar, Department of Computer Science, Kamalam College of Arts and Science, Anthiyur, Affiliated to Bharathiar University, Coimbatore, Tamil Nadu, India,

Email ID: ramya.msc0709@gmail.com

[2] Assistant Professor, Department of Computer Science, Kamalam College of Arts and Science, Anthiyur, Affiliated to Bharathiar University, Coimbatore, Tamil Nadu, India,

Email ID: Kokilamanikcas1@gmail.com

Cite this paper as: Ramya.K, Dr. M.Kokilamani, (2025) Improved Empirical Wavelet Transform Based Signal Preprocessing And Attention-Based Residual Optimized Bilstm (AROBILSTM) Classifier For Epileptic Seizure Detection. *Journal of Neonatal Surgery*, 14 (32s), 1749-1765.

ABSTRACT

The primary diagnostic procedure for epilepsy is the electroencephalogram (EEG). A human expert often detects epileptic activity. Finding particular patterns in the multi-channel (MC) EEG is the foundation of this detection. When using EEG signals to detect epileptic seizures (ESD), pre-processing is essential. Pre-processing eliminates noise and artifacts to guarantee proper analysis and classification. Their ability for feature extraction (FE) from noisy inputs was thus limited. Numerous attempts are made for automating this time-consuming and challenging task using both traditional and Deep Learning (DL) methods. For signal pre-processing, an Improved Empirical (WT) Wavelet Transform (IEWT) is applied to EEG recordings, and it was suggested in this study. The boundaries are separated from the spectrum in order to execute IEWT. To reconstruct the spectrum's (TC) trend component, IEWT selects several points in the spectrum's Fourier transform (FT). Then, the Improved ResNet-50 model computes the features of EEG signals in a number of specific frequency bands (FB). By incorporating the residual structure and layer normalisation (LN) into a BILSTM, the Attention-based Residual Optimised (BI-LSTM) Bidirectional Long Short-Term Memory (AROBILSTM) network classifier is presented. The accuracy (ACC) and stability of epilepsy detection are eventually improved by this integration. In order to optimise the final feature information, this integration also provides an attention mechanism (AM) and enhances the network's FE capabilities. The outputs of the epilepsy network are further processed utilising seizure merging, threshold (T) comparison, and moving average filtering (MAF) to ascertain whether or not the tested EEG that are related to a seizure. On the scalp EEG database from Children's Hospital Boston-Mass Institute of Technology (CHB-MIT), the suggested approach performed better than alternative methods in terms of precision (P), recall/sensitivity (R/S), F-measure, and accuracy (ACC).

Keywords: *Epileptic seizure detection (ESD), scalp EEG, AROBILSTM network, Improved Empirical Wavelet Transform (IEWT), and ResNet-50 model.*

1. INTRODUCTION

Electrical disturbances in the brain that occur quickly and randomly are a symptom of ES [1], a neurological condition. A group of neurological dysfunctions with a persistent propensity that can lead to repeated seizures is known as epilepsy in neurology [2]. Frequent body convulsions, mind degradation, and cognitive disorders are all signs of an ES. As a result of these ES symptoms, people's quality of life is declining and there are more safety concerns. To treat patients with antiepileptic drugs (AEDs) and lower the risk of future seizures, accurate and early detection (ED) of ES is essential [3]. By examining EEG data, epilepsy patients' typical brain activity is divided into four states.

In seizure detection (SD) research, the epileptic records are usually separated into four distinct stages of brain activity (BA): interictal (IL), preictal (PRL), ictal (ICL), and postictal (POL). The synchronised activity of neurons in numerous brain regions can be shown by this massive amount of data [4]. In recent years, ESD using MC scalp EEG data has gained more attention in the domain of neuro information technology. In order to diagnose epilepsy, neurology specialist typically perform visual assessments on patients in clinics. Additionally, neurologists typically invest a great deal of effort and time in looking for indications of epilepsy in long-term (LT) EEG recordings. Due to their affordability, portability, and distinct frequency-

domain rhythms, EEG signals are commonly chosen [5]. EEG provides the voltage variations brought on by the ionic current of neurons. The bioelectric activity of the brain is indicated by this EEG [6].

Neurophysiologists can make early predictions of upcoming seizures by closely monitoring EEG data, that includes recordings of the brain's electrical activity made with non-invasive (NI) electrodes placed on the scalp. This allows them to examine the BA during both seizure and nonseizure periods. The analysis is complicated by the fact that these signals are recorded across multiple channels. Muscle tremor, electrode movement, and the main power source can all produce artifacts in the EEG readings [7, 8]. Doctors will find it challenging to detect ES from noisy EEG readings as a result. Many studies are being conducted to eliminate noises utilising EWT-based techniques in order to address these challenges. The signal is broken down into frequency components by EWT. By creating a unique wavelet basis, EWT enables in-depth analysis. By extracting the required components from unwanted noise, researchers and practitioners can improve signal analysis. While preserving signal information, the EWT technique successfully removes noise [9, 10].

By employing methods like filtering, denoising, and normalisation to eliminate noise and interference, pre-processing is used to enhance signal quality (SQ). The signal's usability and dependability are enhanced by pre-processing. The pre-processed signal's representative information is extracted as part of FE. The collected features are mapped to specified categories or states using machine learning (ML) and DL techniques. To accomplish precise pattern recognition (PR) and classification, this step entails training and implementing classification models. In terms of differentiating seizure EEG, Support Vector Machine (SVM), Random Forest (RF), and Artificial (NN) Neural Network (ANN) have demonstrated varying performances [11]– [12]. Because the testing data has a different probability distribution than the training data, many classifiers lack the robustness and generalisation capabilities that requires.

The amount of labelled samples and hardware setup are critical requirements for Deep NN (DNN) [13], [14]. Thus, the development of the EEG classifier continues to be one of the research centres in the field of automatic SD (ASD). Nowadays, Convolutional NN (CNN) and BiLSTM are popular. The ability to classify EEG ES and performing outstanding automated FE has been demonstrated by this CNN. Therefore, it is challenging for CNN to re-establish the connection between the raw EEG and the outcomes of ES. Because recurrent NN (RNNs) are trained on previous outputs, they are able to retain historical information. In order to effectively categorise ES, hybrid DL models have proven to be more effective and superior.

For signal pre-processing, the IEWT is applied to EEG recordings. Then, the Improved ResNet-50 model computes the features of EEG signals in a number of specific frequency bands. By incorporating layer normalisation and residual structure into a BiLSTM, the AROBILSTM network classifier is presented. Using the CHB-MIT scalp EEG database, the suggested approach performed better than earlier methods in terms of P, R/S, F-measure, and ACC.

2. LITERATURE REVIEW

An efficient ASD method based on the Stockwell transform (S-transform) and BiLSTM NN was suggested by Geng et al. [12]. The suggested method is specifically made for intracranial EEG recordings.The S-transform is applied first to raw EEG segments. In order to feed the resulting matrix into BiLSTM for FS and classification, it is then organised into time-frequency blocks. To enhance detection performance, postprocessing is then used. MAF, threshold judgement, MC fusion, and collar method are all part of this post-processing. The suggested approach is evaluated using a total of 20 patients' 689-h intracranial EEG recordings. According to the results, there is promising clinical practice potential for the seizure detection (SD) approach.

Instead of using manual FE, Zhou et al. [15] employed a CNN based on raw EEG signals to distinguish between ICL, PRL, and IL segments for ESD. By contrasting the efficacy of time domain (TD) and frequency domain (FD) signals in the identification of epileptic signals based on the scalp CHB-MIT and intracranial Freiburg databases, the suggested approach examined the potential of these factors. Two binary classification (BC) problems (IL vs. PRL and IL vs. ICL) and one three-class problem (IL vs. PRL vs. ICL) were used to examine the feasibility of this strategy. FD signals from the Freiburg database and the average ACC for detection from the CHB-MIT database were used to calculate the average ACC for the three tests. Comparing FD signals to TD signals, the classification ACC of FD signals is generally much higher. Furthermore, for CNN applications, FD signals are more promising than TD signals. A feature vector is created by combining non-EEG information after spectral and spatial features have been extracted. These feature vectors can then be used to train a SVM, which is subsequently used for classification.

FE was made an obligatory step by Shoeibi et al. [16]. The handcrafting features or learning those features with the support of the DNN is then employed for executing the FE. The best features are then selected for signal classification on a benchmark dataset for assessment using Fisher scores. For a thorough comparison of FE techniques, a five-layer convolutional autoencoder (AE) is also used to learn features. For SD in EEG signals, a CNN-AE is used, that integrates handcrafted features with AE encoding.

Based on MC scalp EEG recordings, Yuan et al. [17] suggested a unified multi-view (MV) DL architecture to capture brain anomalies linked to seizures. The suggested method may simultaneously train MV features from supervised SD using spectrogram representation and unsupervised MC EEG reconstruction. A new AE-based MV learning model incorporates

both intra- and intra-correlations of EEG channels. To focus the MV structure on important and relevant EEG channels, a channel-aware SD module was suggested. The training process was then modified by including a channel-wise competition mechanism. The efficacy of the suggested methodology is demonstrated through a thorough study of a benchmark scalp EEG dataset against baselines, which comprises both traditional handcrafted FE methods and standard DL approaches. Using five-fold subject-independent (CV) cross validation, simulation results show that the suggested framework may provide higher average ACC and f1-score, 94.37% and 85.34%. The suggested approach is proving to be an effective way to classify EEG SD.

Using the Fisher vector (FV) encoding and multiscale radial basis function (MRBF) networks, Li et al. [18] developed a unique ASD technique. In particular, the high-resolution (HR) time-frequency (TF) for FE is initially obtained using the MRBF networks. The two optimisation techniques: Orthogonal Least Squares (OLS) and Modified Particle Swarm Optimisation (MPSO) to analyse HD data by identifying ideal scales and a simplified model structure. The influence of FV and Grey Level Co-occurrence Matrix (GLCM) texture descriptors on the HD vectors is the main focus of the analysis.Then, using five frequency subbands of clinical interest from TF, discriminative features are created using these HD vectors. Before introducing compact data into the SVM classifier for SD, the t-test statistical approach may effectively decrease the size of the original feature space. Finally, two well-known EEG database are employed for evaluating the recommended technique's detection ability, and both datasets show good classification ACC. The outcomes of the simulation indicate that the suggested approach is an optimal ESD tool.

In order to identify the ES utilising both the MC scalp and single-channel EEG signals, Reduced Deep Convolutional Stack AE (RDCSAE) and Improved Kernel Random Vector Functional Link Network (IKRVFLN) was suggested by Sahani et al. [19]. The goal of the novel RDCSAE structure is to extract the most discriminative unsupervised features from EEG signals in order to detect the ES activity with possible ACC. The suggested supervised IKRVFLN classifier then receives these features. This suggested supervised IKRVFLN classifier reduces the mean-square error cost function (MSE) to train efficiently. The suggested method is tested using single-channel EEG datasets from Boon University, Germany and the benchmark Boston Children's Hospital MC scalp EEG (sEEG). Reduced computational complexity, faster learning speed, improved model generalisation, accurate ESD, remarkable classification ACC, negligible FP rate per hour (FPR/h), and short event recognition time are the primary advantages of the suggested approach over reduced deep CNN (RDCNN), RDCSAE, and RDCSAE-KRVFLN methods.

Li et al. [20] designed an end-to-end (E2E) EEG SD architecture using a novel channel-embedding spectral-temporal squeeze-and-excitation network (CE-stSENet) with a maximum mean discrepancy (MMD) -based information maximising loss (IML). The first to combine multi-scale temporal analysis and multi-level spectral analysis at the same time is the CE-stSENet. Hierarchical multi-domain representations are then coherently captured using a squeeze-and-excitation block variation.Based on FE in earlier subnetworks, classification is used for epileptic EEG recognition. A MMD-based IML is integrated with the CE-stSENet to mitigate the severe overfitting problem in SD, which is caused by a lack of seizure events. It will lead to a finite data distribution. The performance of the recommended model in detecting epileptic EEGs is demonstrated by experimental findings on three EEG datasets compared to the state-of-the-art (SOTA) methods. The suggested technique validates its strong ability in the ASD.

A new SD technique based on the deep Bi-LSTM network was presented by Hu et al. [21]. The nonstationary quality of EEG signals is preserved and the processing load is decreased with the incorporation of statistical FE methods and local mean decomposition (LMD). Next, two separate LSTM networks with opposing propagation directions are combined to create the deep architecture. Information is sent from the front (f) to the back (b) via one and from the b to the f via another. The output state can thus be simultaneously determined by the deep model by utilising the information both before and after the currently analysed moment. A mean specificity (SP) of 91.85% and a mean S of 93.61% were found on an LT scalp EEG database. The enhanced performance for SD was shown by comparing with previous published techniques based on CNN or conventional ML models.

In order to effectively detect seizure onsets, a novel patient-independent (PI) method was suggested by Liu et al. [22]. First, the MC EEG signals are preprocessed using wavelet decomposition (WD). After that, the CNN functions as an EEG FE with the appropriate depth. The temporal variation features are then further captured by inputting the acquired features into a BiLSTM network. At last, the model's outputs undergo post-processing, which includes collar and smoothing, in order to lower the False Detection Rate (FDR) and increase the S. To improve the model's capacity for generalisation, a unique channel perturbation technique is introduced throughout training. Using average ACC, average S, and average Area Under the Receiver Operating Characteristic Curve (AUC-ROC), both the Second Hospital of Shandong University (SH-SDU) scalp EEG dataset and the CHB-MIT public scalp EEG dataset are used for evaluating the efficacy of the suggested method.

An automatic spatial–temporal (S-T) ESD framework based on DL has been suggested by He et al. [23]. In particular, the front-end for extracting spatial features is graph attention networks (GAT). The structure of several EEG channels is thus fully utilised. The BiLSTM network is used as the back-end to mine time relations and make the final decision based on the state before and after the present moment. The studies are conducted using the CHB-MIT and Temple University Hospital

(TUH) datasets. According to comprehensive experimental results, the proposed method may effectively detect seizures from the raw EEG signals without the requirement for further FE. The suggested method executes superior than SOTA methods.

In order to diagnose epilepsy from EEG signals, the convolutional LSTM (ConvLSTM) based the deep ST NN was suggested by Tawhid et al. [24]. The suggested framework first selects and resamples standard 19-channel EEG data at 256 Hz. Next, 3-s time frames are used to separate the signals. The ConvLSTM model then uses the segmented data as input to distinguish epileptic patients from healthy individuals. The experiment's biases are eliminated using leave-one-out CV (LOOCV) schemes and five-fold CV. For the examined datasets, the simulation outcomes show that the suggested approach executes superior than the existing SOTA outcomes. The suggested approach qualifies it as an automated system for epilepsy diagnosis.

Quadri et al., [25] proposed a series of 1-D convolution layers (CL), each with several filters with lengths varying exponentially. The deep Bi-LSTM layers are subsequently integrated to the design to create a densely connected feed-forward structure. The model effectively prioritizes ST information, thus extracting key insights for identification of interictal and preictal features. The proposed model has undergone comprehensive evaluations, with S, P, F1-Score, and an AUC-ROC. CHB-MIT dataset is utilized and fivefold CV is applied for training the model.

Bidirectional gated recurrent unit (Bi-GRU) NN is an ASD technique that Zhang et al. [26] introduced to help with epilepsy diagnosis and treatment. First, EEG data are pre-processed and filtered using WT. Initially, a Bi-GRU network receives the relative intensities of the EEG signal in a certain FB. To ascertain whether the EEG data corresponds to a seizure, the Bi-GRU's output is then further refined using MAF, threshold comparison, and seizure merging. The CHB-MIT scalp EEG database outcomes indicate that the Bi-GRU network performs better in SD. For LT EEG monitoring, the recommended detection technique may be beneficial.

3. PROPOSED METHODOLOGY

For signal pre-processing, IEWT is introduced in EEG signals. The boundaries are separated from the spectrum in order to execute IEWT. To reconstruct the spectrum's TC, IEWT selects various points in the spectrum's FT. Then, the Improved ResNet-50 model computes the features of EEG signals in a number of specific FB. By incorporating layer normalisation (LN) and residual structure into a BiLSTM, the AROBILSTM network classifier is presented. Through this integration, the network's FE capabilities are improved, an AM is included to optimise the final feature information, and the ACC and stability of epilepsy detection are finally improved.

Compared to previous approaches, the CHB-MIT database was used to analyse metrics like classifying R/S, F-measure, and ACC as well as problems in ASD. The general procedure of the suggested model is depicted in Figure 1.

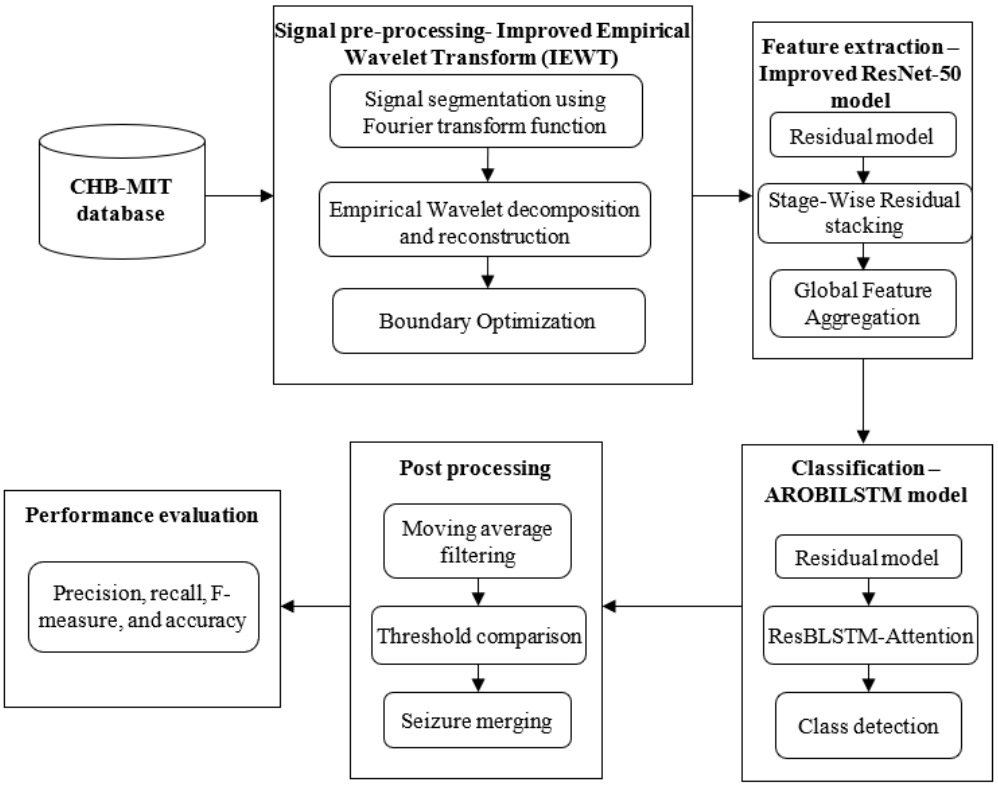

FIGURE 1. OVERALL FLOW OF PROPOSED MODEL

3.1 Signal Pre-Processing based Improved (EWT) Empirical Wavelet Transform (IEWT)

The vibration acceleration signal can be adaptively broken down into a number of empirical modes using EWT. The following three steps can be used to describe the EWT method: (1) segment the spectrum adaptively, (2) based on the boundaries, a suitable EW (Empirical wavelet) filter bank was created. Then, the signal is filtered and (3) Using the Hilbert transform (HT), the empirical modes are reconstructed, demodulated, and assessed [27].

Step 1: Split the boundaries in the FD

The EEG signal's FD is split into N FB with varying bandwidths (BW) after being normalised to [0, π]. Instead of employing Gilles' technique, the boundary requirement is the midway of the adjacent maxima. The boundaries of each FB in the EEG signal are identified using the spectral (TE) trend estimation (STE) approach, which is based on the key function.

Step 2: Create an EWT filter bank

Gilles decided to use the Meyer wavelet (MWT) as the basis function to generate an EW. During the transition phase, a set of orthogonal trigonometric functions is produced. Here, a constant is created in the FB and the FB boundary is identified.

Step 3: Execute an EWT

The FT is F(.), and the inverse FT (IFT) is F(.). The EWT transform is defined using a methodology akin to the conventional WT. Spectrum segmentation and border optimisation are two of EWT's flaws that are examined and explained. By determining the spectrum's FT function, a novel IEWT technique determines the spectrum's TC. The EEG signal is reconstructed using the minimum points of the TC as boundaries. Different TC will be reconstructed by choosing different points in key functions (KF). Reasonable EWT boundaries can be obtained with an appropriate TC. The following are the precise stages:

Phase 1: The EEG signals with periodic impacts $y(t)$ are collected. The spectrum $\Upsilon(f)$ is obtained using the Fast FT (FFT) technique. Further, the FFT approach yields the key function $K(f)$, which is the FT function of $\Upsilon(f)$.

Phase 2: To inverse the FT and reconstruct the spectrum's TC $\left(T_c(f)\right)$, a specific amount of points are taken out of the K(f). The spectrum will be split into multiple sections when more points are used to reconstruct the complicated TC since there will be more extreme points in the TC. The reconstructed function is close to the trend of spectrum changes, and the spectrum will be split up into fewer pieces.

Phase 3: Determine and optimise the spectrum's boundaries. The minimum point sequence serves as the boundary array, with the TC serving as the basis function. The wavelet threshold optimises the boundary array when the TC is complicated. To a certain degree, the invalid components produced by noise are reduced using the technique of optimising spectrum boundaries based on threshold denoising (TD) of the EEG signal.

Phase 4: Use EWT to carry out signal processing (SP). Select MWT as the basis function after normalising the signal's FD into [0,π]. This MWT constructs adaptive filters (AF), divides the signal into its constituent parts, and defines the empirical scaling function $\phi_n(\omega)$ and the empirical wavelets $\Psi_n(\omega)$.

- **TE Technique depends on the KF**

The trend of the spectrum can be reconstructed using the suggested method's TE step based on the KF. The theoretical basis of the FT is integrated into this approach. The algorithm is more efficient than the conventional EWT. This algorithm has a faster computation time than an interpolation algorithm.

Phase 1: In equation (1), the FFT algorithm is used for obtaining the FB of the estimaed signal

$$\mathbf{\Upsilon(f) = FFT(y(t))} \quad (1)$$

Phase 2: Use equation (2) to determine the FT function of Y(f).

$$\mathbf{K(f) = FFT\ \Upsilon(f)} \quad (2)$$

Phase 3: Equation (3) establishes a close relationship between the spectrum and the KF components.

$$\mathbf{T_c(f) = iFFT\left(K_B(f)\right)} \quad (3)$$

Here, $T_c(f)$ is a TC and $K_B(f)$ is the left portion of boundary B in K(f). The TC resembles a straight line, as TC is soft, and fluctuates very little. When there are fewer reconstructed points than the initial maximum value of the KF B_1, this TC is not obvious from the spectrum fluctuation pattern.

The spectrum of the EEG signal is split into two areas by one minimum. There is a lot of information in the first area. This first region does not separate the spectrum's appropriate frequency components. The thirty-point reconstruction of the TC is

bounded by the minimum values. A cluster of modulation data with a side band in the spectrum is displayed by the impact and modulation components. As a result, while handling EEG signals, the TE approach based on the KF provides advantages. Selecting too many EEG signals from the KF for the inverse transformation (IT) will result in a rough partition that can hold the modulation data with side-band frequency but cannot separate the information with close frequency. To a certain degree, the suggested approach can retain and eliminate the unnecessary elements. Some details, such as the elements having spectra exist near to each other, can be retrieved from simulation EEG signals when several points are chosen for IT; however, this will result in an excessive number of areas in the spectrum. To address these problems, the threshold noise-reduction (TNR) technique is presented [28].

- **TD method**

Wavelet TD is the main application for TD. The wavelet coefficients (WC) are recovered from the original EEG signal.This WC are obtained via wavelet decomposition (WD). The coefficients are then denoised. Different threshold functions (TF) have an impact on the reconstruction outcomes as well as the denoising effect during the TD process. When estimating data, setting the threshold is crucial. The noise-induced spectrum fluctuation must be minimised during the TD process because this method does not have to fully display the trend. The hard TF by equation (4) [28] is one of the often-utilised TF.

$$\hat{\mathbf{s}} = \begin{cases} \mathbf{s}|\mathbf{s}| \geq \boldsymbol{\lambda} \\ \mathbf{o}|\mathbf{s}| < \boldsymbol{\lambda} \end{cases} \tag{4}$$

Using equation (5) for the soft TF,

$$\hat{\mathbf{s}} = \begin{cases} \mathbf{sgn(s)}.(|\mathbf{s}| - \boldsymbol{\lambda})|\mathbf{s}| \geq \boldsymbol{\lambda} \\ \mathbf{o}|\mathbf{s}| < \boldsymbol{\lambda} \end{cases} \tag{5}$$

Here, the EEG signal to be processed is denoted by s. The EEG signal after denoising is represented by $\hat{s}$.Then, a fixed threshold of λ is offered by this $\hat{s}$ [29].

$$\boldsymbol{\lambda} = \boldsymbol{\sigma}\sqrt{\mathbf{2In(N)}} \tag{6}$$

The equation (6) required signal length is denoted as N. The estimated noise variance is denoted by σ^2. The reconstructed signal (RS) oscillates at the discontinuity point due to the discontinuity of s at λ and - λ. But, the hard T can effectively retain the signal's local data during processing. Soft threshold processing improves the overall continuity of ˆs. Even yet, there is a constant discrepancy between s and $\hat{s}$, and the derivatives are discontinuous. This could have an impact on the reconstruction ACC. This approach may ignore these soft threshold defects and just requires the spectrum trend. The threshold (T) used to process the signal sequence is $\lambda = 0.5\mathrm{m/s^2}$. The graph makes the good continuity of soft thresholds very evident. There are local steps in the hard thresholds.

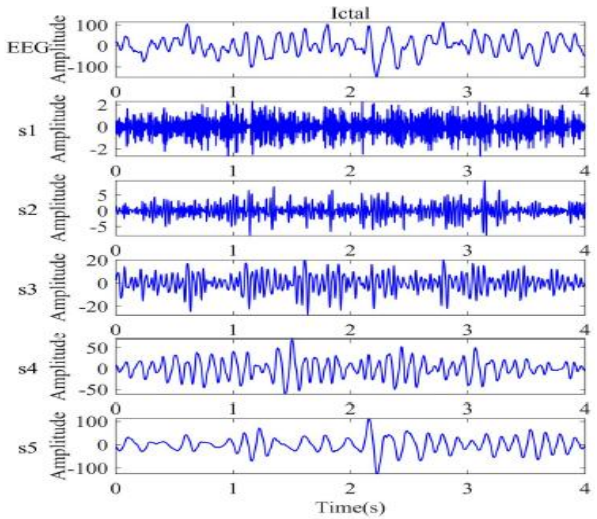

FIGURE 2. SEGMENT OF ICTAL EEG AND ITS RECONSTRUCTED SIGNALS.

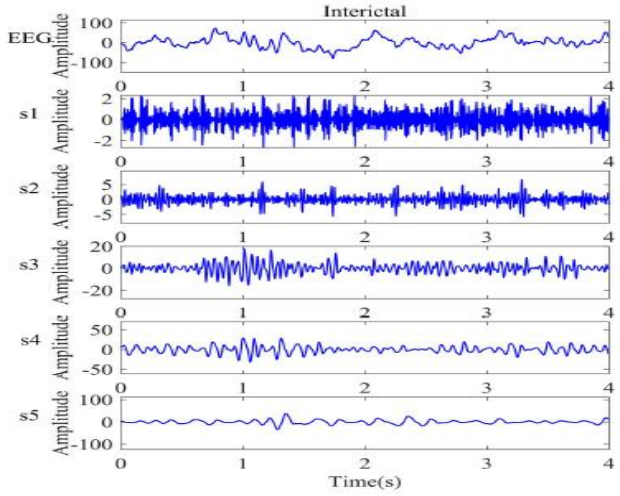

FIGURE 3. SEGMENT OF INTERICTAL EEG AND ITS RECONSTRUCTED SIGNALS

Two EEG segments and their RS are shown in Figures 2 and 3. The ictal and interictal EEG signals are displayed in the upper panels of Figures 2 and 3, respectively. The RS on scales 1 to 5 are represented as s1 to s5, following WD and reconstruction on five scales. Figures 2 and 3 demonstrate the clear amplitude variations among the two EEG classes in the RS on scale 3 to 5.

3.2 FE based Improved ResNet-50 NN

The introduction of skip connections (SC) is one of the main characteristics of the ResNet-50 FE model. By using identity mappings (IM), these SC enable input EEG signals to pass through one or more layers and pass directly to next layers. The gradient vanishing problem (GVP) has been effectively solved using this SC. Instead of learning a mapping function directly, the network can learn the residual from the input and output via ResNet. This method improves training efficiency and FE capability by ensuring that the network's performance doesn't deteriorate when depth increases. Training deeper networks is now possible due to ResNet. ResNet enables steady training performance and efficient gradient flow maintenance for models with hundreds or even thousands of layers.

The components of the improved ResNet-50 model include a fully connected (FC) layer, four groups of residual layers, a global average pooling (GAP) layer, a batch normalisation (BN) layer, a ReLU (AF) activation function, a 3×3 max (PL) pooling layer (MPL) , and a M×N CL. The input EEG signal is directly added to the output in this design using residual blocks (RB) with SC. This integration improves training stability and FE while effectively minimising the GVP in deep networks. The subsequent sections offer a thorough description of the model construction and training procedure based on this network structure [30].

- **Initial CL**

Equation (7) illustrates how to first pre-process the input ECG signal and calculate the related input tensor.

$$\mathbf{X} \in \mathbf{R}^{\mathbf{N\times 3\times H\times W}} \tag{7}$$

Here, the batch size is denoted by N. Samples supplied into the NN during each training iteration are denoted by N. The image height is denoted as H. The image width is represented as W. The pre-processing of the image data is finished after the input tensor is acquired. The DL network is adequately ready for FE, gradient propagation, and optimisation due to this pre-processing. The image data is then subjected to the M × N convolution (Conv) operation. Equation (8) expresses its mathematical formulation.

$$\mathbf{Y} = \mathbf{W} * \mathbf{X} + \mathbf{b} \tag{8}$$

Here, each Conv kernel's parameters are denoted as W. After the (Conv) process, Y is the output feature map (FM). The bias term is indicated by b. Equations (9-10) computes the dimensions of convolutional output FM.

$$\mathbf{H'} = \frac{\mathbf{H+2p-k}}{\mathbf{s}} + \mathbf{1} \tag{9}$$

$$\mathbf{w'} = \frac{\mathbf{w+2p-k}}{\mathbf{s}} + \mathbf{1} \tag{10}$$

About half of the original size of the FM's spatial dimensions is lost in the ECG signal, after the M×N Conv, and it can be seen from the calculations above. In order to guarantee a more stable activation distribution and promote the network's convergence, each FM channel are then independently normalized. Equation (11) provides the normalisation for each channel of the FM output by the M × N Conv.

$$\hat{\mathbf{x}}_\mathbf{i} = \frac{\mathbf{x_i} - \boldsymbol{\mu}_\mathbf{B}}{\sqrt{\boldsymbol{\sigma}_\mathbf{B}^2 + \boldsymbol{\epsilon}}} . \boldsymbol{\gamma} + \boldsymbol{\beta} \tag{11}$$

Here, the variance and mean of each channel in the current batch are denoted by σ_B^2 and μ_B. Learnable parameters are γ and β. FM go via the ReLU AF after the FM of each channel has been normalised. The purpose of the ReLU function is to suppress negative activation values while improving the ResNet-50 model's nonlinear (NL) representation capacity. Enhancing model sparsity and enabling more efficient feature learning are two benefits of the ReLU function. After that, the FM size is further reduced by applying a 3×3 max PL. According to equation (12), down sampling (DS) specifically uses a 3×3 pooling kernel with a stride of 2.

$$y_{ij} = \max_{m,n\in\{0,1,2\}} x_{(2i+m)(2j+m)} \quad (12)$$

The MPL further reduces the FM's spatial dimensions to half of the Conv output FM, according to calculations.

- **Residual Module (RM) Design**

Three CL and one SC make up each residual block in an improved ResNet-50 network model. Restoring the number of channels, extracting spatial features, and lowering computational complexity are the three CL tasks. The SC then enhances deep network training's stability and learning potential, mainly addressing the GVP. The RB's computational procedure is explained in the part that follows [31]. Two 1×1Conv and one 3×3 spatial Conv make up the three CL.

The 1×1 dimension reduction Conv processes the EEG data by first computing the input tensor using equation (13-14). Here, $X_1 \in \mathbb{R}^{N\times C_{mid}\times H\times W}$. is the output of executing steps in Equation (14). $X_2 \in \mathbb{R}^{N\times C_{mid}\times H'\times W'}$ is the output of calculating the FM's 3×3 spatial Conv by equation (15). Then, utilising Equation (16), the resultant FM is processed through a 1×1 expansion Conv. $X_3 \epsilon R^{N\times C_{out}\times H'\times W'}$ is the final output obtained by restoring the number of channels using a scaling factor (SF) of 4.

$$C_{mid} = \left\lfloor C_{out} \times \frac{width}{64} \right\rfloor \quad (13)$$

$$X_2 = W_2 * X_1 + b_2 \quad (14)$$

Here, $H' = \frac{H}{2}, W' = \frac{W}{2}$, a stride of s = 2 is used in this experiment. The computed outcomes are given below the equation (15)

$$X_3 = W_3 * X_2 + b_3 \quad (15)$$

The key component of the ResNet network model is the residual connection. It overcomes the difficulties of deep network training by employing cross-layer SC. Preventing VGP, improving information flow, and boosting optimisation performance are the main purposes of residual connections. Equation (16) provides a basic formulation.

$$Y = \mathcal{F}(X, \{W_i\}) + X \quad (16)$$

Here, the input FM is represented by X. The final output is immediately skipped over X. The first three CL are FM derived from the EEG signal, which is denoted by $\mathcal{F}(X, \{W_i\})$. The final output EEG signal FM is denoted by the Y. On the other hand, When the stride is 2, the FM size is halved, resulting in an output size of $\frac{H'}{2} + \frac{W'}{2}$ from an input size of H×W. Because of their mismatched spatial dimensions, the input X in this instance cannot be applied directly to $\mathcal{F}(X)$.

These steps are used to address this using DS residual connections. In order to enable element-wise addition, the input X is first adjusted using a 1×1 Conv to match $\mathcal{F}(X)$ in shape. D espite extending the receptive area, DS between stages aids in lowering computational complexity. The FM's spatial dimensions shrink as the number of channels rises with each stage transition. As a result, more abstract and high-level (HL) features can be processed by deeper network layers without considerably rising processing costs. Furthermore, a wider receptive field aids in capturing more contextual data, improving the model's capacity for global perception.

- **Stage-Wise (SW) Residual Stacking (RS)**

The EEG signal is recorded using the SW ResNet-50 model. Higher detection ACC is attained by the SW ResNet-50 model. To improve the seizure model's feature learning capabilities, stacking RB has been implemented. The stride is kept at 1 in the next blocks, but it is set to 2 in the first RB of each stage for DS in order to maximise computing efficiency. Computational complexity is effectively decreased by this method. This technique balances variations in the number of channels while enlarging the receptive field. Additionally, the potential of the framework in effectively training and extracting seizure-associated attributes at various levels is ensured [31].

- **Global Feature Aggregation (GFA) and Classification**

The network eventually generates an output FM of size $X_{stage} \in \mathbb{R}^{N\times 2048\times m\times n}$ after stacking the RB across four stages. Global information modelling is improved with the application of GFA to further process this FM. Every m×n ECG signal FM is specifically compressed to a 1×1 size using Equation (17). This compression preserves the channel dimension information and ensuring that global information is effectively aggregated. Consequently, $Y_{pool} \in \mathbb{R}^{N\times 2048\times 1\times 1}$. is the size of the final output FM.

$$y_c = \frac{1}{m \times n} \sum_{i=1}^{m} \sum_{j=1}^{n} x_{cij} \tag{17}$$

The pooled output of the c^{th} channel is denoted by y_c. In the c^{th} channel, x_{cij} represents the feature value at row i and column j. The output from equation (18) needs to be flattened because the FC layer can only take one-dimensional inputs. Specifically, the flattened function from the Torch library is used. A flattened FM of $Y_{flat} \in \mathbb{R}^{N \times 2048}$ will result from this. An FC layer is used to map the 2048-dimensional feature vector into a 7-dimensional ECG category prediction vector.

$$Z = W_{fc} Y_{flat} + b_{fc} \tag{18}$$

Here, the weight matrix of the FC layer is represented by $W_{fc} \in \mathbb{R}^{N_{classes} \times 2048}$. The bias term is then indicated as $b_{fc} \in \mathbb{R}^{N_{classes}}$. Unnormalized classification scores are represented by $Z \in \mathbb{R}^{N \times N_{classes}}$. In order to transform the logits into a probability distribution for every class, the classification scores determined in EQN (19) must be further processed using the Softmax function after being unnormalized. The normalised Pi is guaranteed to satisfy $\sum_{i=1}^{N_{classes}} P_i = 1$ by the computation provided by Equation (20).

$$P_i = \frac{e^{z_i}}{\sum_{j=1}^{N_{classes}} e^{z_j}} \tag{19}$$

Here, z_i is a representation of the sample's logit score for class i. P_i is the expected probability that the sample belongs to class i.

3.3 Classification based AROBILSTM

The AROBILSTM serves as the basis for SD. The three main parts of the network structure are depicted in Figure 4. They are: improved ResNet-50, ROBILSTM, and Attention. The EEG signal's signal features are extracted by the first component, Improved Resnet50. The ROBILSTM component enhances the framework's capacity to identify LT dependencies in the EEG signal by fusing the advantages of BILSTM with residual connections. To further improve the final detection, AM is added.

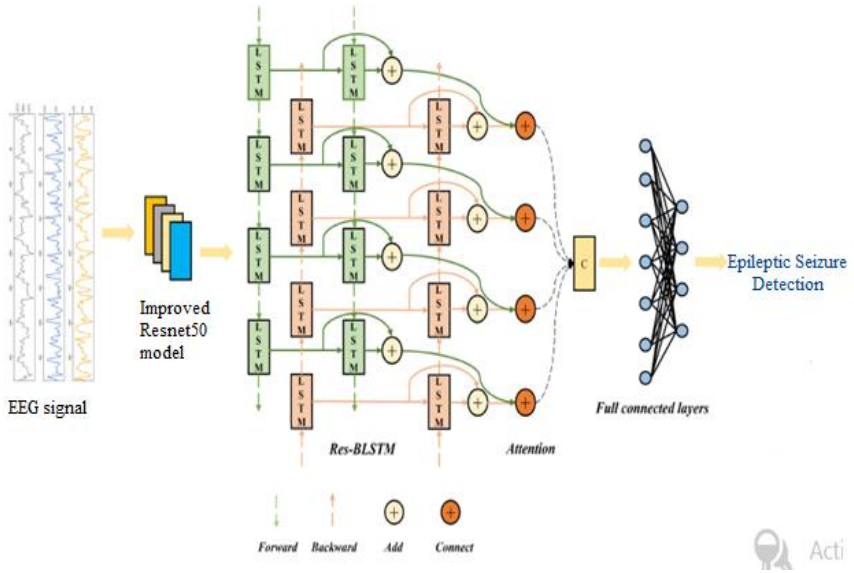

FIGURE 4. AROBILSTM MODEL

- **ROBILSTM**

Both forward (F) and backward (B) information are considered by the two-way LSTM network known as BILSTM. By capturing bidirectional relationships, BILSTM improves FE when compared to the LSTM network. Thus, it is appropriate to use a BILSTM network to extract signal properties from an EEG signal [32–33].

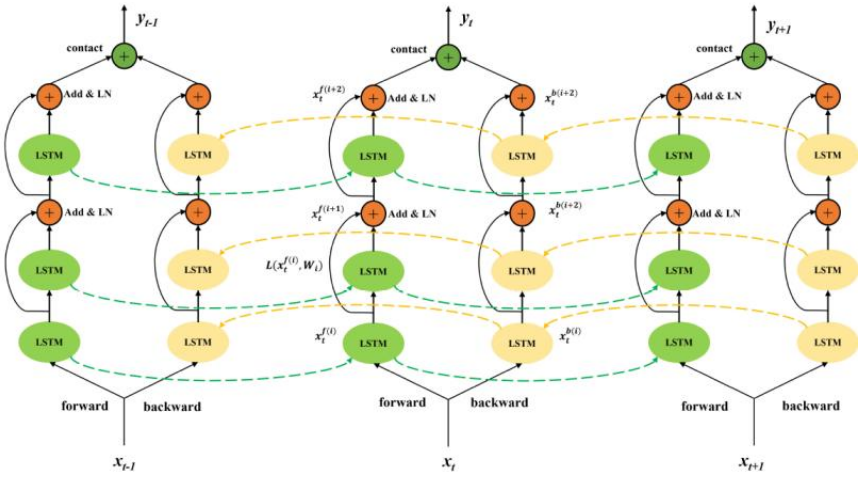

FIGURE 5. ROBILSTM MODEL

The ROBILSTM network is made up of F and B LSTM networks, as seen in Figure 5. The final encoding information is then combined into the F and B states once each LSTM has been added to the ResNet and LN. Figure 6 displays the unique residual structure.

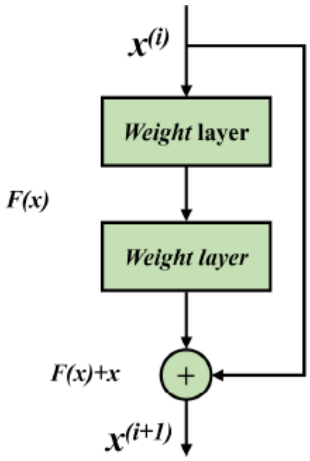

FIGURE 6. RB OF RESNET50 MODEL

Equation (20) can be used to express every RB.

$$\mathbf{x^{i+1} = x^{i} + F(x^{i}, w_{i})} \quad (20)$$

Here, x^{i} is a direct mapping, the RB are separated into two parts. The residual part is denoted as $F(x^{i}, w_{i})$. Likewise, the encoder component of the Transformer model is designed using the previously discussed structure. Based on the advantages of this structure, research provides a ResNet based on the BILSTM network. In the BILSTM network, normalisation techniques can also be applied. Compared to BN, LN is especially beneficial for RNN. It is calculated similarly to BN and may be written in the following way with the equation (21):

$$\mathbf{z^{(i)} = \frac{x^{(i)} - E(x^{(i)})}{\sqrt{var(x^{(i)})}}} \quad (21)$$

Here, the input vector for the i dimension is denoted by $x^{(i)}$. After LN, the output is represented as $z^{(i)}$. As seen in Figure 5, a new combination known as ROBILSTM is presented, that combines ResNet and LN in a BILSTM network. The recursive feature information y is expressed as equation (22-24):

$$\mathbf{x_t^{f(i+1)} = LN\left(x_t^{f(i)} + L\left(x_t^{f(i)}, w_i\right)\right)} \quad (22)$$

$$\mathbf{x_t^{b(i+1)} = LN\left(x_t^{b(i)} + L\left(x_t^{b(i)}, w_i\right)\right)} \quad (23)$$

$$\mathbf{y^t = concat\left(x_t^f, x_t^b\right)} \quad (24)$$

Here, layer normalisation is denoted by LN. In the LSTM network, L is the processing of input states. The t^{th} moment in the EEG signal is indicated by the subscript t in $x_t^{f(i+1)}$. The F state is denoted by the f in the superscript, and the B state by b. Here, (i+1) is the number of stacked layers, and the encoded data y_t at time t is spliced together from the F state and the B state.

- **AM**

Specific parts of the input EEG signal can be the focus of an AM in DL. Different elements are given varying weights by AM. The weight of the recursive data y produced by ROBILSTM is determined to be α. The final feature information C is obtained by multiplying and adding each weight α to y.

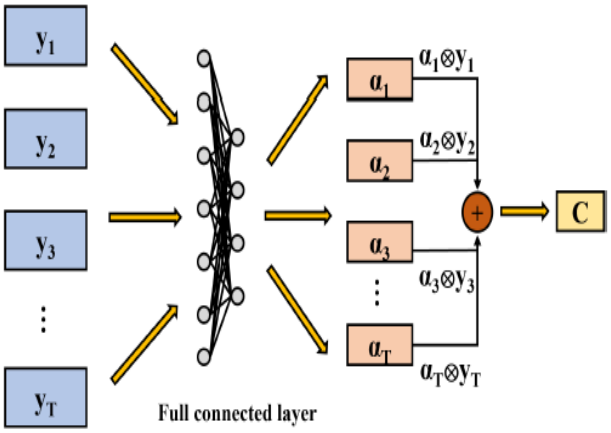

FIGURE 7. AM

The FE calculation approach is explained as follows the equation (25), and it is presented in Figure 7:

$$\mathbf{e_t = f(y_t), \alpha_t = \frac{exp(e_t)}{\sum_{i=1}^{T} exp(e_i)}, C = \sum_{t=1}^{T} \alpha_t y_t} \quad (25)$$

Here, back propagation (BP) across the FC layer can be used to learn the function f expression. Throughout the training process, the weight α_t is continuously changing, and the feature information C gets more representational as training goes on.

- **Optimization Mechanism**

One effective method for tuning the hyperparameters (HP) in the BILSTM model is Bayesian Optimisation (BO). By creating a probabilistic model of the objective function (OF), it effectively explores the HP space. BO directing the search for configurations that show promise. Set the training epoch count to 150 and the learning rate to 0.001. Set the batch size to 64 because of the computer's memory limitations. The model incorporates dropout to avoid overfitting. To prevent excessively employing computing resources by excessive fine-tuning (FT), other HP are kept relatively unaltered.

4. RESULTS AND DISCUSSION

With an i7 CPU, 16GB of RAM, and an NVIDIA RTX3050 GPU, MatlabR2019a was used to apply the ESD techniques. The testing data from every case in the CHB-MIT database was used to assess the SD approaches' efficiency.

4.1 Database

The Children's Hospital Boston collected the CHB-MIT scalp EEG database from https://physionet.org/content/chbmit/1.0.0/. The International 10-20 system of EEG electrode locations, with a sampling rate of 256 Hz and 16 bits resolution, was employed in the EEG data collecting process. EEG recordings from 23 epileptic patients

were gathered and categorised into 24 cases in the CHB-MIT database. Cases chb21 and chb01 were extracted from the same subject one and a half years apart. The majority of continuous EEG files (which vary from 9 to 42) consist of 1 hour of EEG signals, with the exception of a few files from cases chb04, chb06, chb07, chb09, chb10, and chb23, that are 2-4 hours duration.

The CHB-MIT Scalp EEG Database currently contains the EEG recordings of 22 paediatric subjects who had unexpected seizures. In order to describe seizures and find whether the subjects were candidates for surgery, they were observed for a few days after stopping anti-seizure medication. Annotated are the beginnings and endings of 198 seizures in total. In the training dataset, the non-seizure (NS) EEG might resemble the seizure (S) EEG by a factor of two to four. A total of around 198.14 minutes of EEG recordings were used as training data for the 24 cases in Table 1.

TABLE I. CHB-MIT EEG DATASET

Case	Gender	Age	Number of Seizures
chb01	F	11	7
chb02	M	11	3
chb03	F	14	7
chb04	M	22	4
chb05	F	7	5
chb06	F	1.5	10
chb07	F	14.5	3
chb08	M	3.5	5
chb09	F	10	4
chb10	M	3	7
chb11	F	12	3
chb12	F	2	40
chb13	F	3	12
chb14	F	9	8
chb15	M	16	20
chb16	F	7	10
chb17	F	12	3
chb18	F	18	6
chb19	F	19	3
chb20	F	6	8
chb21	F	13	4
chb22	F	9	3
chb23	F	6	7
chb24	-	-	16
Total	-	-	198

4.2 Performance assessment

Evaluation metrics such as P, R/S, F-measure, and ACC are used to assess how well the SD methods perform. The following formulas can be used to determine each of these evaluation criteria (26–29).

$$\mathbf{P} = \frac{\mathbf{TP}}{\mathbf{TP} + \mathbf{FP}} \tag{26}$$

$$\mathbf{R} = \frac{\mathbf{TP}}{\mathbf{TP} + \mathbf{FN}} \tag{27}$$

$$\mathbf{F-measure} = \frac{\mathbf{2 \times P \times R}}{\mathbf{P + R}} \tag{28}$$

$$\mathbf{ACC} = \frac{\mathbf{TP + TN}}{\mathbf{TP + FP + TN + FN}} \tag{29}$$

The number of S and NS segments that the detection system accurately detects is referred to as True Positive (TP) and True Negative (TN). The number of non-seizure EEG segments that the detection system mistakenly interprets as seizure is known as False Positive (FP). Seizures with incorrect labels are known as false negatives (FN).

TABLE 2. PERFORMANCE COMPARISON OF SOME SD APPROACHES

APPROACHES	P (%)	R (%)	F-MEASURE (%)	ACC (%)
CONVLSTM	83.25	86.63	84.91	85.22
BI-LSTM	85.57	87.79	86.67	86.83
BI-GRU	87.38	89.52	88.44	88.21
S-TRANSFORM WITH BILSTM	89.76	90.87	90.31	89.78
CE-STSENET	91.51	92.88	92.19	91.54
AROBILSTM	93.65	94.23	93.94	93.57

The performance comparison of SD approaches like ConvLSTM, Bi-LSTM, Bi-GRU, S-transform with BiLSTM, CE-stSENet, and AROBILSTM with respect to P, R, F-measure, and ACC are shown in Table 2.

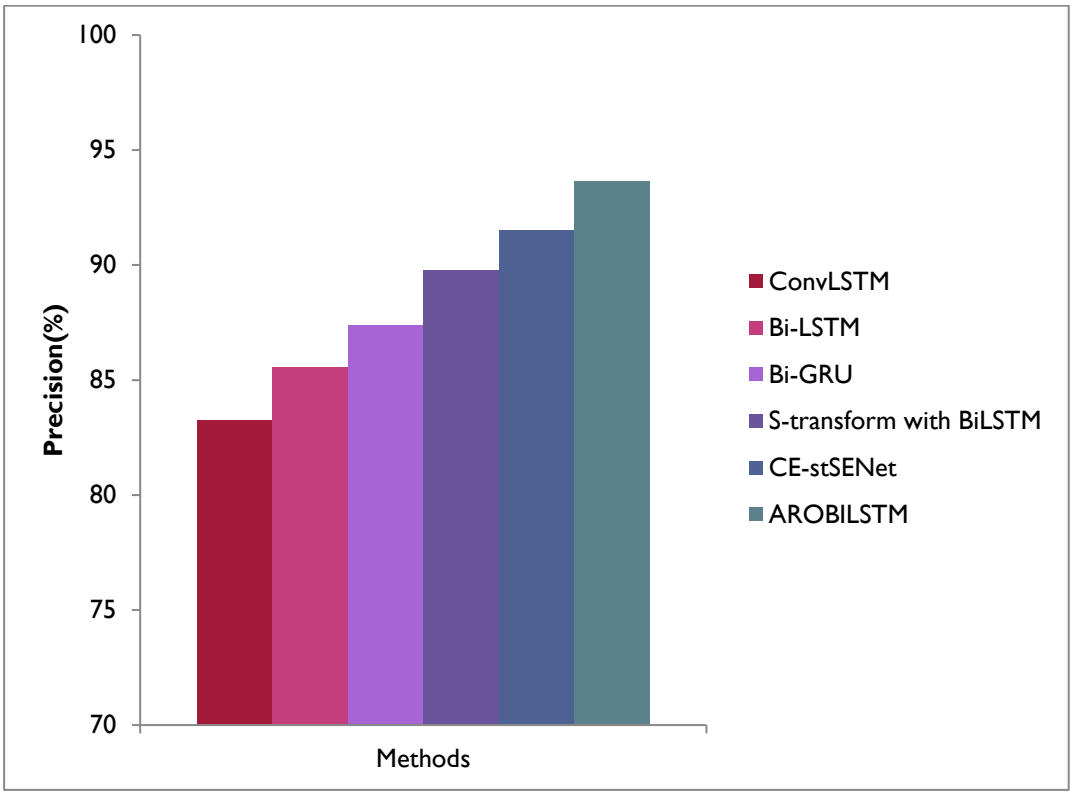

FIGURE 8. PRECISION COMPARISON OF SEIZURE DETECTION METHODS

Figure 8 shows the precision results comparison of seizure detection methods like ConvLSTM, Bi-LSTM, Bi-GRU, S-transform with BiLSTM, CE-stSENet, and AROBILSTM. It shows that the proposed classifier has highest results of 93.65%, other methods such as ConvLSTM, Bi-LSTM, Bi-GRU, S-transform with BiLSTM, CE-stSENet gives some lowest results of 83.25%, 85.57%, 87.38%, 89.76%, and 91.51%.

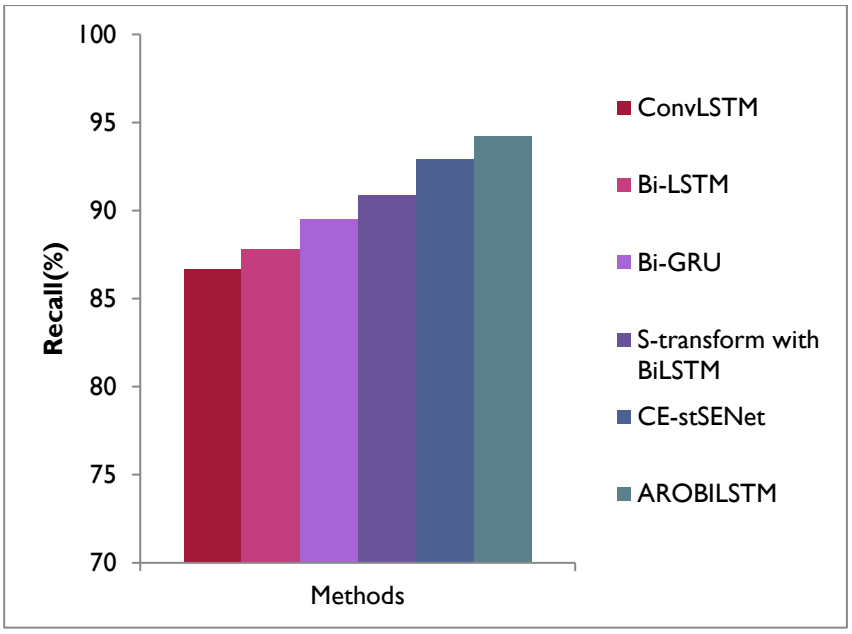

FIGURE 9. RECALL COMPARISON OF SEIZURE DETECTION METHODS

Figure 9 shows the recall results comparison of seizure detection methods like ConvLSTM, Bi-LSTM, Bi-GRU, S-transform with BiLSTM, CE-stSENet, and AROBILSTM. It shows that the proposed classifier has highest results of 94.23%, other methods such as ConvLSTM, Bi-LSTM, Bi-GRU, S-transform with BiLSTM, CE-stSENet gives some lowest results of 86.63%, 87.79%, 89.52%, 90.87%, and 92.88%.

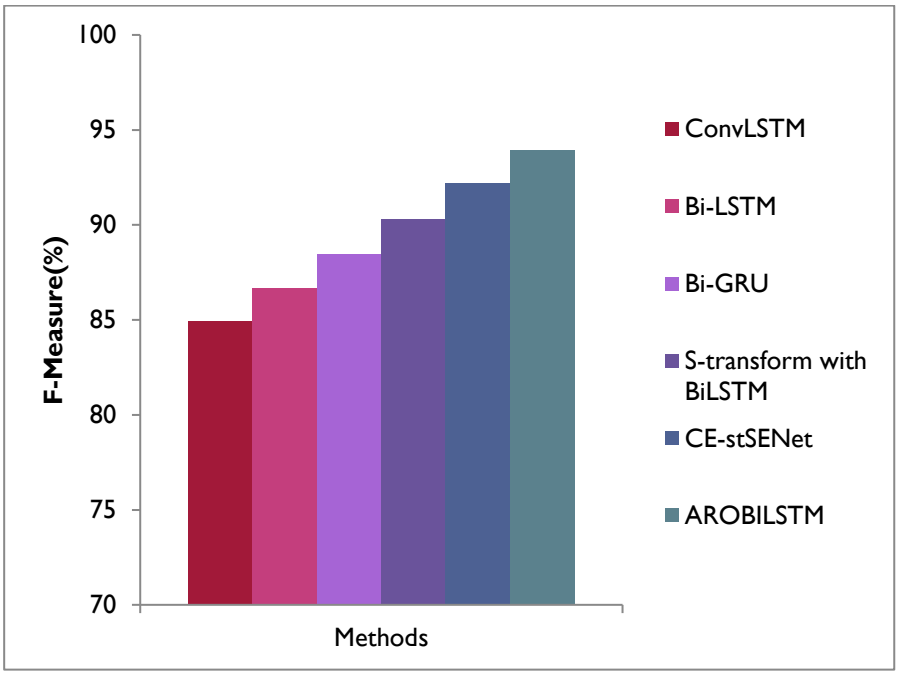

FIGURE 10. F-MEASURE COMPARISON OF SEIZURE DETECTION METHODS

F-Measure comparison of seizure detection methods like ConvLSTM, Bi-LSTM, Bi-GRU, S-transform with BiLSTM, CE-stSENet, and AROBILSTM are illustrated in figure 10. It shows that the proposed classifier has highest results of 93.94%, other methods such as ConvLSTM, Bi-LSTM, Bi-GRU, S-transform with BiLSTM, CE-stSENet gives some lowest results of 84.91%, 86.67%, 88.44%, 90.31%, and 92.19%.

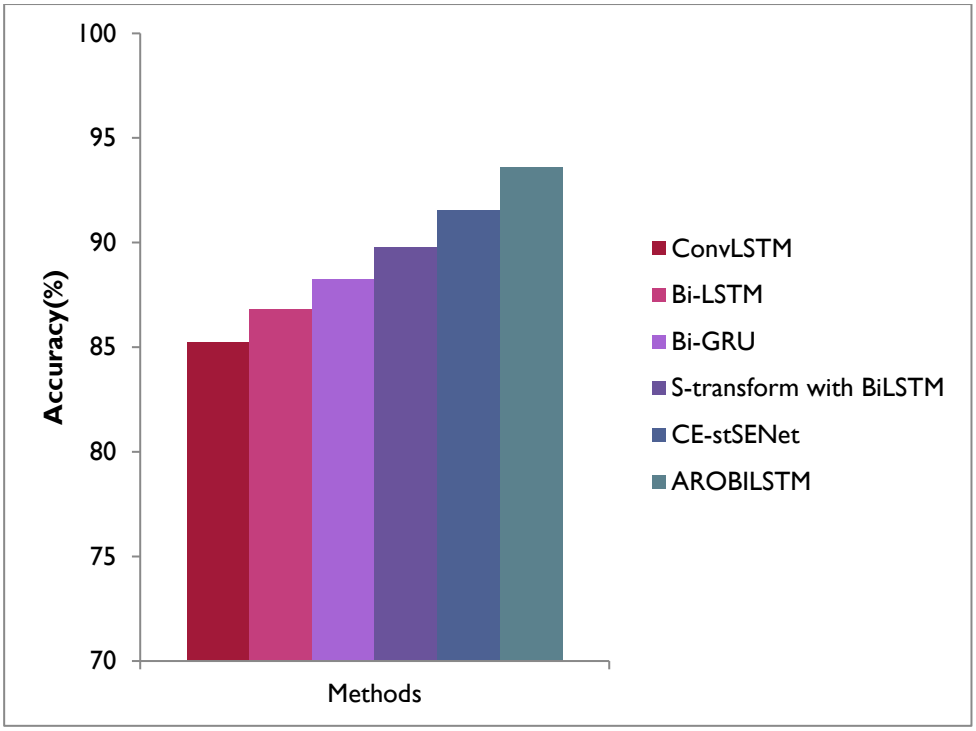

FIGURE 11. ACC COMPARISON OF SD APPROACHES

Accuracy comparison of SD approaches like ConvLSTM, Bi-LSTM, Bi-GRU, S-transform with BiLSTM, CE-stSENet, and AROBILSTM are illustrated in figure 11. It indicates that the suggested classifier has highest results of 93.57%, other methods such as ConvLSTM, Bi-LSTM, Bi-GRU, S-transform with BiLSTM, CE-stSENet gives some lowest results of 85.22%, 86.83%, 88.21%, 89.78%, and 91.54%.

5. CONCLUSION AND FUTURE WORK

This SD presented makes use of an AROBILSTM NN and time-frequency analysis of EEG components. EEG recordings from children with uncontrollable seizures are included in the CHB-MIT dataset. By tackling noise and TC, signal pre-processing techniques such as IEWT and TNR are employed to improve signal quality. With a TE based on a KF, IEWT seeks to recover the trend of the signal. The goal of TNR is to eliminate noise artifacts. RB with SC is used in an improved ResNet-50 model, which is very helpful for FE from EEG signals. By directly adding the input EEG signal to the output of the RB, these linkages enhance training stability and FE capabilities. The purpose of stacking RB is to enhance the seizure model's feature learning capabilities. The residual structure and LN are integrated into a BILSTM to introduce the AROBILSTM network classifier. Among AROBILSTM is ResNet-50. Signal FE from the EEG signal is the responsibility of this ResNet-50. The ROBILSTM component develops the framework's capacity to identify LT dependencies in the EEG data by fusing the advantages of BILSTM with residual connections. To further optimise the model, AM and BO are also added. On the CHB-MIT dataset, evaluation measures such as P, R, F-measure, and ACC are used to compare the outcomes of the suggested model to current detection techniques. The number of EEG electrodes has no effect on the suggested detection method. Future studies are needed to see whether this recommended method heps specific epilepsy patient in offering an effective detection model. Promoting detection effectiveness in PI applications and real-time clinical EEG data with more noise and artifacts should be the main goals of future research.

REFERENCES

[1] Vidyaratne, L.S. and Iftekharuddin, K.M., 2017. Real-time epileptic seizure detection using EEG. IEEE Transactions on Neural Systems and Rehabilitation Engineering, 25(11), pp.2146-2156.

[2] Bhattacharyya, A., Pachori, R.B., Upadhyay, A. and Acharya, U.R., 2017. Tunable-Q wavelet transform based multiscale entropy measure for automated classification of epileptic EEG signals. Applied Sciences, 7(4), pp.1-18.

[3] Kulaseharan, S.; Aminpour, A.; Ebrahimi, M.; Widjaja, E. Identifying lesions in paediatric epilepsy using morphometric and textural analysis of magnetic resonance images. Clin. NeuroImage 2019, 21, pp.1-8.

[4] Zazzaro, G., Cuomo, S., Martone, A., Montaquila, R.V., Toraldo, G. and Pavone, L., 2021. EEG signal analysis

for epileptic seizures detection by applying data mining techniques. Internet of Things, 14, pp.1-17.

[5] Chakrabarti, S.; Swetapadma, A.; Pattnaik, P.K. A review on epileptic seizure detection and prediction using soft computing techniques. In Smart Techniques for a Smarter Planet; Springer: Cham, Switzerland, 2019; pp. 37–51.

[6] Liu, X.Y., Wang, W.L., Liu, M., Chen, M.Y., Pereira, T., Doda, D.Y., Ke, Y.F., Wang, S.Y., Wen, D., Tong, X.G. and Li, W.G., 2025. Recent applications of EEG-based brain-computer-interface in the medical field. Military Medical Research, 12(1), pp.1-42.

[7] Kedadouche, M., Thomas, M. and Tahan, A.J.M.S., 2016. A comparative study between Empirical Wavelet Transforms and Empirical Mode Decomposition Methods: Application to bearing defect diagnosis. Mechanical Systems and Signal Processing, 81, pp.88-107.

[8] Zheng, J.D.; Pan, H.Y.; Yang, S.B. Adaptive parameterless empirical wavelet transform based time-frequency analysis method and its application to rotor rubbing fault diagnosis. Signal Process. 2017, 130, 305–314.

[9] Liu, W. and Chen, W., 2019. Recent advancements in empirical wavelet transform and its applications. IEEE Access, 7, pp.103770-103780.

[10] Elouaham, S., Dliou, A., Jenkal, W., Louzazni, M., Zougagh, H. and Dlimi, S., 2024. Empirical wavelet transforms based ECG signal filtering method. Journal of Electrical and Computer Engineering, 2024(1), pp.1-13.

[11] Wei Z., J. Zou, J. Zhang, and J. Xu, "Automatic epileptic EEG detection using convolutional neural network with improvements in time-domain," Biomed. Signal Process. Control, vol. 53, Aug. 2019, Art. no. 101551, pp.1-11.

[12] Geng M., W. Zhou, G. Liu, C. Li, and Y. Zhang, "Epileptic seizure detection based on stockwell transform and bidirectional long shortterm memory," IEEE Trans. Neural Syst. Rehabil. Eng., vol. 28, no. 3, pp. 573–580, Mar. 2020.

[13] Rashed-Al-Mahfuz, M., Moni, M.A., Uddin, S., Alyami, S.A., Summers, M.A. and Eapen, V., 2021. A deep convolutional neural network method to detect seizures and characteristic frequencies using epileptic electroencephalogram (EEG) data. IEEE journal of translational engineering in health and medicine, 9, pp.1-12.

[14] Prabin Jose J., M. Sundaram, and G. Jaffino, "Adaptive rag-bull rider: A modified self-adaptive optimization algorithm for epileptic seizure detection with deep stacked autoencoder using electroencephalogram," Biomed. Signal Process. Control, vol. 64, Feb. 2021, Art. no. 102322, pp.1-11.

[15] Zhou, M., Tian, C., Cao, R., Wang, B., Niu, Y., Hu, T., Guo, H. and Xiang, J., 2018. Epileptic seizure detection based on EEG signals and CNN. Frontiers in neuroinformatics, 12, pp.1-14.

[16] Shoeibi, A.; Ghassemi, N.; Alizadehsani, R.; Rouhani, M.; Hosseini-Nejad, H.; Khosravi, A.; Panahiazar, M.; Nahavandi, S. A comprehensive comparison of handcrafted features and convolutional autoencoders for epileptic seizures detection in EEG signals. Expert Syst. Appl. 2021, vol.163, no.113788, pp.1-16.

[17] Yuan Y., G. Xun, K. Jia, and A. Zhang, "A multi-view deep learning framework for EEG seizure detection," IEEE J. Biomed. Health Inform., vol. 23, no. 1, pp. 83–94, Jan. 2019.

[18] Li Y., W.-G. Cui, H. Huang, Y.-Z. Guo, K. Li, and T. Tan, "Epileptic seizure detection in EEG signals using sparse multiscale radial basis function networks and the Fisher vector approach," Knowl.-Based Syst., vol. 164, pp. 96–106, Jan. 2019.

[19] Sahani, M., Rout, S.K. and Dash, P.K., 2021. Epileptic seizure recognition using reduced deep convolutional stack autoencoder and improved kernel RVFLN from EEG signals. IEEE transactions on biomedical circuits and systems, 15(3), pp.595-605.

[20] Li, Y., Liu, Y., Cui, W.G., Guo, Y.Z., Huang, H. and Hu, Z.Y., 2020. Epileptic seizure detection in EEG signals using a unified temporal-spectral squeeze-and-excitation network. IEEE Transactions on Neural Systems and Rehabilitation Engineering, 28(4), pp.782-794.

[21] Hu, X., Yuan, S., Xu, F., Leng, Y., Yuan, K. and Yuan, Q., 2020. Scalp EEG classification using deep Bi-LSTM network for seizure detection. Computers in Biology and Medicine, 124, pp.1-8.

[22] Liu, G., Tian, L. and Zhou, W., 2022. Patient-independent seizure detection based on channel-perturbation convolutional neural network and bidirectional long short-term memory. International journal of neural systems, 32(06), pp.1-17.

[23] He J., J. Cui, G. Zhang, M. Xue, D. Chu, and Y. Zhao, "Spatial–temporal seizure detection with graph attention network and bi-directional LSTM architecture," Biomedical Signal Processing and Control, vol. 78, no.103908,

pp.1-9, 2022.

[24] Tawhid M. N. A., S. Siuly, and T. Li, "A convolutional long short-term memory-based neural network for epilepsy detection from EEG," IEEE Transactions on Instrumentation and Measurement, vol. 71, pp. 1–11, 2022.

[25] Quadri, Z.F., Akhoon, M.S. and Loan, S.A., 2024. Epileptic Seizure Prediction using Stacked CNN-BiLSTM: A Novel Approach. IEEE Transactions on Artificial Intelligence, vol.5, no.11, pp. 5553 – 5560.

[26] Zhang, Y., Yao, S., Yang, R., Liu, X., Qiu, W., Han, L., Zhou, W. and Shang, W., 2022. Epileptic seizure detection based on bidirectional gated recurrent unit network. IEEE Transactions on Neural Systems and Rehabilitation Engineering, 30, pp.135-145.

[27] Liu, W. and Chen, W., 2019. Recent advancements in empirical wavelet transform and its applications. IEEE Access, 7, pp.103770-103780.

[28] Bhattacharyya, A., Sharma, M., Pachori, R.B., Sircar, P. and Acharya, U.R., 2018. A novel approach for automated detection of focal EEG signals using empirical wavelet transform. Neural Computing and Applications, 29, pp.47-57.

[29] Xu, Y., Zhang, K., Ma, C., Li, X. and Zhang, J., 2018. An improved empirical wavelet transform and its applications in rolling bearing fault diagnosis. Applied sciences, 8(12), pp.1-24.

[30] Wen, L., Li, X. and Gao, L., 2020. A transfer convolutional neural network for fault diagnosis based on ResNet-50. Neural Computing and Applications, 32(10), pp.6111-6124.

[31] Yadav, R.K., Mishra, A.K., Saini, J.B., Pant, H., Biradar, R.G. and Waghodekar, P., 2024. A Model for Brain Tumor Detection Using a Modified Convolution Layer ResNet-50. Indian Journal of Information Sources and Services, 14(1), pp.29-38.

[32] Siami-Namini, S., Tavakoli, N. and Namin, A.S., 2019, The performance of LSTM and BiLSTM in forecasting time series. In 2019 IEEE International conference on big data (Big Data), pp. 3285-3292.

[33] Cheng, J., Zou, Q. and Zhao, Y., 2021. ECG signal classification based on deep CNN and BiLSTM. BMC medical informatics and decision making, 21, pp.1-12.